# Miniaturised bidirectional acoustic tag to enhance marine animal tracking studies

Ivan Masmitja
SARTI Research Group, Electronics
Department Universitat Politècnica de
Catalunya
Barcelona, Spain
ivan.masmitja@upc.edu

Daniel Corregidor
Instrumentation and Applied Acoustics
Research Group (I2A2). ETSI
Industriales. Universidad Politécnica de
Madrid. Madrid, spain
daniel.corregidor@i2a2.upm.es

Juan Manuel López
Instrumentation and Applied Acoustics
Research Group (I2A2). ETSI
Industriales. Universidad Politécnica de
Madrid. Madrid, spain
juanmanuel.lopez@upm.es

Enoc Martinez
SARTI Research Group, Electronics
Department Universitat Politècnica de
Catalunya
Barcelona, Spain
enoc.martinez@upc.edu

Joan Navarro
Institut de Ciències del Mar - CSIC
Barcelona, Spain
joan@icm.csic.es

Spartacus Gomariz
SARTI Research Group, Electronics
Department Universitat Politècnica de
Catalunya
Barcelona, Spain
spartacus.gomariz@upc.edu

*Abstract*—**Acoustic underwater tags are key devices to study marine animals and comprehend their patterns, which provide essential behavioural information for applying new conservation policies. At present, all the acoustic tags have a unidirectional communication protocol, which introduces important limitations for their localisation such as range measurement, and in situ reconfiguration. To solve these issues and improve the current state-of-the-art acoustic tags, a new bidirectional tag device is presented in this paper. This innovative tag will allow new studies and will open a wide tracking capability by using autonomous underwater vehicles and range-based algorithms. Here, the main architecture of the tag, and its characteristics are presented alongside the first laboratory tests, and the results obtained.**

*Keywords—Bidirectional, acoustics, tags, underwater, communications, autonomous underwater vehicles, marine species, target localization*

## I. INTRODUCTION

Acoustic underwater tags have an important role to study marine animal behaviour. For example, these tags are crucial to track the movements of underwater species (e.g. Norway lobsters or Snow crabs) and comprehend their patterns, such as light influence [1], diel cycles [2], and long migrations [3]. These studies provide essential behavioural information for applying new conservation policies [4].

For this purpose, miniaturised off-the-shelf tags are usually chosen for many studies [5]. For example, the V7 series from Vemco/Innovasea (Nova Scotia, Canada) or the IBT series from Sonotronics (Arizona, USA). These tags are widely employed, which are used in many studies (e.g. [6] and reference therein). Nonetheless, the increasing needs for scientists and biologists to study more complex behaviours,

and the implications of the human actions in the environment (i.e. climate change [7], ocean acidification [8] or fishing exploitation [9]), have led to the development of new technologies and strategies. These have pushed the boundaries of traditional tracking methods such as presence/absence detections and long baseline (LBL) systems [10].

In addition, other studies have focused on the development of new tags, which have been specifically designed to accomplish challenging tasks. For example, in [11] the authors proposed a flexible and stretchable skin-like tag, or in [12] where a soft-bodied invertebrate eco-sensor tag is presented. Nonetheless, these tags work as dataloggers, and must be recovered to download the information, or the animal must reach the surface to have access to it through land-based wireless communications (i.e. Bluetooth or satellite). Others, such as [13], [14] have focused on piezoelectric transducers design to maximise acoustic tag performance.

At present, all the acoustic tags have a unidirectional communication protocol (i.e. the tag transmits an acoustic signal, which is recorded by a receiver, but cannot receive any signal by an external device). This characteristic introduces important limitations such as: (i) the impossibility to configure the tag after the deployment; (ii) the difficulty to compute the distance between the tag and the receiver (i.e. the time of flight (TOF)), and therefore, range-based target tracking methods are not possible [15], [16]; and (iii), the limitation of tag intercommunication, which could difficult the implementation of acoustic underwater networks, and use the tagged species as mobile nodes.

To improve the current state-of-the-art of electronic tags, we propose a bidirectional tag device which will allow more accurate studies and will open a new wide tracking capability using autonomous underwater vehicles and range-based algorithms. Moreover, thanks to the embedded microprocessor, the tag could also be used to create an underwater wireless sensor network (UWSN) [17], enabling IoT applications and swarm concepts [18].

## II. HARDWARE DEVELOPMENT OF BIDIRECTIONAL TAGS

The main part of the bidirectional tag is detailed in Fig. 1, where a block diagram is presented. The main goal behind this design is to provide a small size and low powered consumption tag, without renouncing a high computational capability. To accomplish that, each component has been chosen carefully, and a strict power management system has been designed.
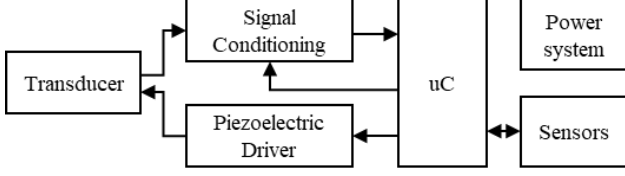


Fig. 1.   Block diagram of the bidirectional tag hardware.

### A. Piezoelectric transducer

Different piezoelectric transducers have been tested to observe their performance. Their size is limited by tag size restrictions, which has maximum dimensions equal to 10x33 mm. The piezoelectric transducers under study were:

- MEGGITT sensing systems: OD10. TH2. PZ29. Screen printed silver (Navy Type VI)
- MEGGITT sensing systems: OD10. TH0.75 PZ29. Screen printed silver (Navy Type VI)
- PI miCos Iberia: Disc OD9. TH3. (Navy Type VI)
- PI miCos Iberia: Plate X15. Y6. TH1.2. (Navy Type I)
- APC International, Ltd.: OD10. TH2. X10. (Navy Type II)

where OD is the external diameter, X and Y are the side dimensions, and TH is the thickness (all dimensions in mm).

### B. Analog signal conditioning system

The analog signal conditioning has been divided into three parts: (i) a preamplifier using the MAX9638 (Maxim Integrated, USA) operational amplifier in a voltage mode configuration; (ii) an attenuator network using a JFET (TF414, ON Semiconductor, USA) as a voltage-controlled resistor; and (iii) a band pass filter (BPF) using another MAX9638. Thus, the final voltage is a function of the voltage applied to the JFET, which is controlled by the microcontroller. Consequently, if the microcontroller's analog to digital converter (ADC) is saturated, the microcontroller can attenuate the signal using this close-loop. A simplified schematic diagram of this system can be observed in Fig. 2.
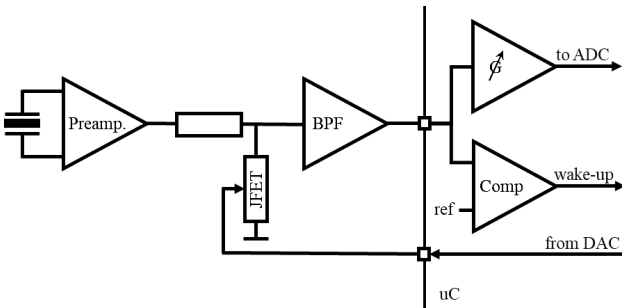


Fig. 2.   Analog signal conditioning circuit, which is composed by a preamplifier with a gain equal to 10, an attenuation network composed by a JFET as a voltage-controlled resistor, a BPF, and a microcontroller (µC) built in operational amplifier, which has adjustable gain, and a comparator used to generate the wake-up signal.

Using this configuration, the total gain of the system is given by

$$V_{ADC} = V_{piezo}\big(G_{preamp} \times Att_{JFET} \times G_{BPF} \times G_{uC}\big), (1)$$

where $G_{preamp} = 10$ is the preamplifier gain, $0.02 < Att_{JFET} \leq 1$ is the attenuation factor introduced by the JFET network, $G_{BPF} = 10$ is the gain of the BPF, and $G_{\mu C} = \{1, 10\}$ is the variable gain introduced by the microcontroller built-in operational amplifier. Therefore, the maximum gain introduced by the circuit is set to 1000, and the minimum is equal to 2.

### C. Digital system

The main part of the digital system consists of a microcontroller (STM32L432KCU6, ST Microelectronics, USA). This is an ultra-low-power microcontroller, with a floating-point unit (FPU) Arm cortex-M4 MCU, with a full set of digital signal processor (DSP) instructions. Moreover, it is packed in a UFQFPN-32 footprint with only 5x5x0.55 mm.

In addition, different sensors can be added. For example, an electronic compass module (LSM303AGRTR, ST Microelectronics, USA) has been introduced in this first version, which has an ultra-low power 3D accelerometer and magnetometer. This is connected to the microcontroller through an I²C serial bus interface.

The microcontroller is in charge to implement the communication protocol, and all the functionalities desired for the tag, such as range measurement between two devices. Nevertheless, in order to extend its life as much as possible, the microcontroller remains in sleep mode for most of the time, and it is only running when an acoustic wake-up signal is detected.

### D. Piezoelectric driver

The piezoelectric driver is in charge to boost the transmission signal generated by the microcontroller in order to maximise the acoustic signal transmitted by the piezoelectric, as well as its efficiency. In this case, a mono 2.6W Class D amplifier (MAX98300, Maxim Integrated, USA) is used. This is a low-powered, ultra-thin footprint amplifier designed for piezoelectric speakers. This amplifier has an efficiency of 89% and uses a bridge-tied-load configuration to multiply the amplifier's voltage-swing capability.

### E. Power management system

Finally, the power system used in the Tag is divided into two elements: (i) two zinc-air batteries (PR41, Duracell, USA) which features a nominal voltage of 1.4 V with a 175 mAh capacity. This button shaped battery has a 7.9 mm diameter and a height of 3.6 mm; and (ii) a hall sensor-switch to turn on/off the tag, which is composed of an omnipolar magnetic latch sensor (CT832BV, Crocus Technology, USA) and a load switch (TCK107AG, Toshiba, Japan). Both devices also have an ultra-low power consumption and a small footprint factor. This magnetic switch is used to turn off the tag using an external manet while it is not in use.

## F. Printed circuit board

The printed circuit board (PCB) designed is presented in Fig. 3A (3D model) and Fig. 3B (manufactured result), which has a final dimension of 33.5x10x0.4 mm, and a weight of 0.2 g in air.
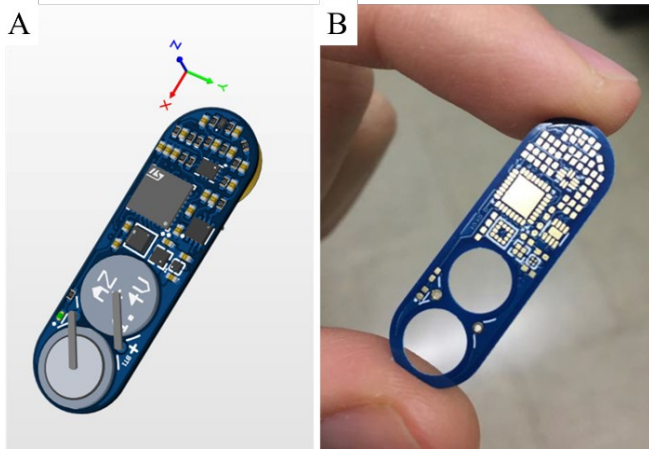


Fig. 3. (A) SASES V2 bidirectional tag 3D model, and (B) the PCB manufactured, which have a size of 33.5x10x0.4 mm.

## III. SOFTWARE IMPLEMENTED IN BIDIRECTIONAL TAGS

The main characteristics of the software are detailed in this section, such as communication protocol and pre-defined functionalities.

### A. Communication protocol

Under the standard communication configuration, a master/slave multidrop protocol [19] in a polling-based transmission scheme [20] is implemented in the tags. The master initiates all communication transactions. Each slave has a unique identification (id), and therefore, it only responds when it is addressed by the master. The master unit can be another tag, or an acoustic modem configured for this purpose.

The standard frame sent by the tag can be observed in Fig. 4, which consists of: (i) a 5 ms chirp signal centred at 50 kHz (10 kHz bandwidth), which is used to wake up the device; (ii) a second chirp signal to generate a high accuracy reception timestamp and to synchronise the tag; (iii) the tag's id number to communicate with; (iv) the information sent, such as the sensor's measurements, tag's status, or the user's commands; and finally, (v) an error checksum to detect possible errors during the transmission.

### B. Modulation

Different modulations have been tested through simulation using the *arlpy* python package, based on the *Bellhop* beam/ray trace code of *Acoustic Toolbox* package. Finally, a frequency-shift keying (FSK) modulation has been chosen, which has a great relation between robustness in front of a reduced signal to noise ratio (SNR) and simplicity to be implemented in small microcontrollers. See [21] for more information.
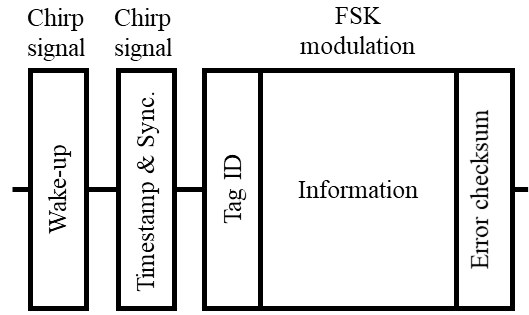


Fig. 4. Information frame transmitted/received by the tag. This consists of: a wake-up chirp signal followed by a blanc space; a second chirp signal, also followed by a blanc space, to timestamp the received frame and the tag's synchronisation; the main body composed by the id of the tag receiver, and the information sent; and finally, an error checksum system.

### C. Pre-defined functionalities

Finally, three different pre-defined functionalities have been configured to use the tags, which are described below:

- Polling-based transmission: The master unit initiates the communication by sending a query to a single tag or to multiple units, which reply with the desired information using their slot times.

- Silent mode transmission: The tags are programmed to transmit a framed information every fixed period of time. In this mode, the reception module (i.e. the analog conditioning system) is turned off. Consequently, this is the lowest consumption mode, and can be used to extend the tag's life.

- Mixed mode transmission: This is a combination between the polling-based and silent modes. The tag is in silent mode most of the time. Nonetheless, after it sends an acoustic message, the reception module is not shut down immediately. Thus, the master unit has a time window to interrogate the tag.

One of the most important aspects of these functionalities and protocols is the tag's power consumption, which depends on the number of subsystems powered, and the tag transmission period. The main power consumption system among functionalities is the analog signal conditioning, which can be operative at a high performance all the time (in Polling mode) or always in low power (LP) as in Silent mode. Furthermore, the tag transmission period is critical in the Silent mode, where the tag life is proportional to the period between the tag's pings.

The tag's life, as a function of the transmission's period and the three modes of communication, is presented in Fig. 5 and summarised in Table 1 (values obtained using laboratory tests). For example, the tag life time can range between 80 to 370 days, for Polling-based and Silent modes respectively. In addition, the Mixed transmission mode consumption, and therefore the maximum life expectancy of the tag, is a function of the time that the analog signal conditioning block is powered on. For example, if the tag is waiting for a master transmission for 10 s (Mixed mode), the tag's maximum life is 230 days for a tag transmission period of 60 s.
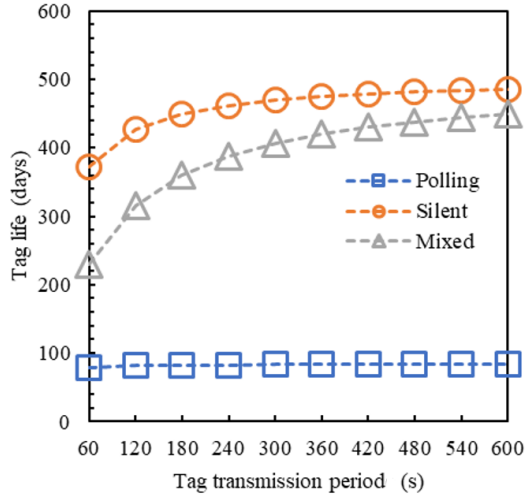
Fig. 5. Tag life time comparison among different functionalities (i.e. Polling-based, Silent, and Mixed mode transmission) and tag transmission period between the tag's pings.

## IV. LABORATORY TEST

The bidirectional tag has been tested in laboratory to characterise its performance in controlled conditions. The results have been obtained employing a test tank (aka a swimming pool) of 2.5x14x1.5 m in dimension, Fig. 6. The most important element under study was the piezoelectric transducers. Different materials and sizes can be found, and in general, piezoelectric transducers with a cylindrical shape have been used [13]. This shape has the advantage of omnidirectional propagation characteristics. Nonetheless, we have opted for disc and plate shapes in order to reduce the thickness of our device, and therefore, the overall volume. This planar form factor has the main issue of a more directional propagation response, but matches the

requirements of our scenario (where we are interested in tracking benthic marine species from above).

The piezoelectric transducers have been compared with a Brüel & Kjaer (Naerum, Denmark) miniature hydrophone type 8103, with a receiving sensitivity of -211 dB re 1V/µPa connected to an amplifier, given an overall sensitivity of -180 dB re 1V/µPa, over the frequency range 0.1 Hz to 200 kHz.

### A. Piezoelectric transducer impedance

The piezoelectric impedance is presented in Fig. 7. In this figure, we can see that below 100 kHz, neither of them has a resonance frequency. A piezoelectric acoustic projector is usually preferred to operate at its resonance frequency for maximum energy output. However, this is not always possible due to size limitations. The resonant frequency for a disc shape is given by [22]



Fig. 6. Test tank of 2.5x14x1.5 m in dimension with a Bruel & Kjaer hydrophone (left) and a piezoelectric transducer under test (right), and the amplifier, signal generator, osciloscope and computer used to conduct the measurements.

TABLE I.   POWER CONSUMPTION AND TAG LIFE TIME AS A FUNCION OF THE DIFFERENT PRE-DEFINED FUNCTIONALITIES: POLLING, SILENT, AND MIXED MODES

| Subsystem | Low Power | Power consumption (µA) | Pre-defined functionalities | | | | | |
|---|---|---|---|---|---|---|---|---|
| | | | Polling | | Silent | | Mixed | |
| | | | % of usage | Total consumption (µA) | % of usage | Total consumption (µA) | % of usage | Total consumption (µA) |
| Analog signal conditioning | ● | 77 | 100 | 77.00 | 0 | 5.00 | 17 | 17.02 |
| | ○ | 5 | 0 | | 100 | | 83 | |
| Microcontroller* | ● | 2688 | 0.17 | 11.56 | 0.17 | 11.56 | 0.17 | 11.56 |
| | ○ | 7 | 99.83 | | 99.83 | | 99.83 | |
| Piezoelectric driver† | ● | 780 | 0.08 | 0.72 | 0.08 | 0.72 | 0.08 | 0.72 |
| | ○ | 0.1 | 99.92 | | 99.92 | | 99.92 | |
| Power management | ● | 0.4 | 100 | 0.40 | 100 | 0.40 | 100 | 0.40 |
| Sensors | ● | 53.7 | 0.01 | 2.01 | 0.01 | 2.01 | 0.01 | 2.01 |
| | ○ | 2 | 99.99 | | 99.99 | | 99.99 | |
| Average power consumption (µA) | | | 91.69 | | 19.69 | | 31.71 | |
| Tag life (days)# | | | 80 | | 370 | | 230 | |

* Microcontroller in low power (LP) stope mode during 100 ms

† 50 ms of tag signal transmission

# based on two PR41 batteries with 175 mAh of capacity

●/○ low power enabled/disabled

$$f_r(radial) = \frac{N_r}{2r}, \; f_r(thickness) = \frac{N_\tau}{\tau}, \qquad (2)$$

where $N_i$ is the frequency constant in the $i \in \{r, \tau, L\}$ direction. This parameter is a function of the shape, the surface finish, and the coupling factor, but in general it is between $1500 \leq N_i \leq 2200$ (Hz m). $r$ is the radii of the piezoelectric, and $\tau$ is its thickness. On the contrary, the resonant frequency for a plate shape is

$$f_r(transverse) = \frac{N_L}{L}, \; f_r(thickness) = \frac{N_\tau}{\tau}, \quad (3)$$

where $L$ is the size dimension of the plate. Therefore, to reduce the resonant frequency, the size of the transducer has to be increased. Nonetheless, this is not feasible because the size of the overall devise must be kept in the required values.

In addition, the signal frequency should be as low as possible in order to reduce underwater acoustic attenuation (which increase with frequency [23]), and to reduce the microprocessor speed, and therefore, its power consumption.
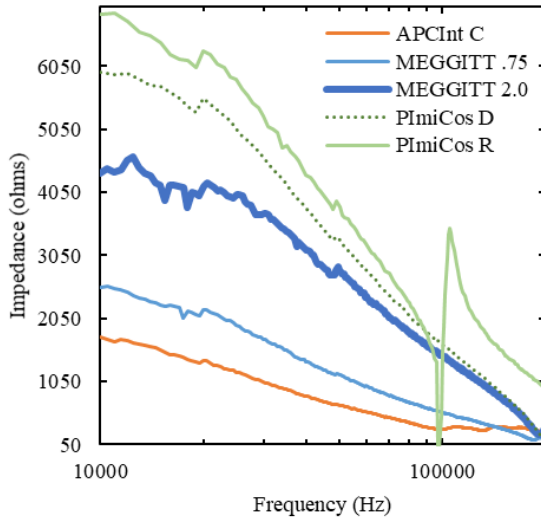


Fig. 7. Impedance measurement for different piezoelectric transducers, which was tested at different frequencies. The PI miCos R (Navy type I) has a resonant frequency at 100 kHz.

### B. Source level

The source level (SL) is the sound power transmitted by the acoustic tag and it is measured as it is in sound pressure level (SPL), which is commonly referenced to 1 m re 1 µPa. If the distance between the source and the sensor is less than 1 m, the following equation can be used, assuming spherical spreading of the acoustic energy, which is an approximation of the sound propagation [23]

$$SL_{1m} = SL_{rec} + 20\log(R), \qquad (4)$$

where $SL_{1m}$ is the sound level at 1m, $SL_{rec}$ is the recorded sound level, and $R$ is the horizontal range in meters between the hydrophone and the sound source.

The maximum range that an acoustic transmission can reach (i.e. can be detected) is function of the SL, the transmission loss (TL) given by

$$TL = 20\log(R) + \alpha R, \qquad (5)$$

where $\alpha$ is the absorption loss which follows a linear law with respect to the distance (e.g. ~17.5 dB/km at 50 kHz [24]), and

the ambient noise. Usually, a signal to noise ratio (SNR) level of 10 dB is a sufficient margin for most of the modulations. Consequently, the desired minimum SL to reach a specific range R is defined by

$$SL \geq TL + NL + SNR, \qquad (6)$$

where $NL$ is the noise level (e.g. ~56 dB re 1 µPa for a Beaufort Scale wind force 6 and 50 kHz of signal frequency [23]).

Eq. 6 yields in a desired SL equal to 115.5 dB re 1 µPa at 1m and frequency of 50 kHz to ensure sufficient detection range (i.e. at least 200 m) and efficiency in noisy environments.

Finally, the SL measured using the piezoelectric transducers under study can be observed below. The transducers were located at 0.5 m from the Brüel & Kjaer hydrophone, and their performance measured under different voltage amplitudes and frequencies, Fig. 8 and Fig. 9 respectively.
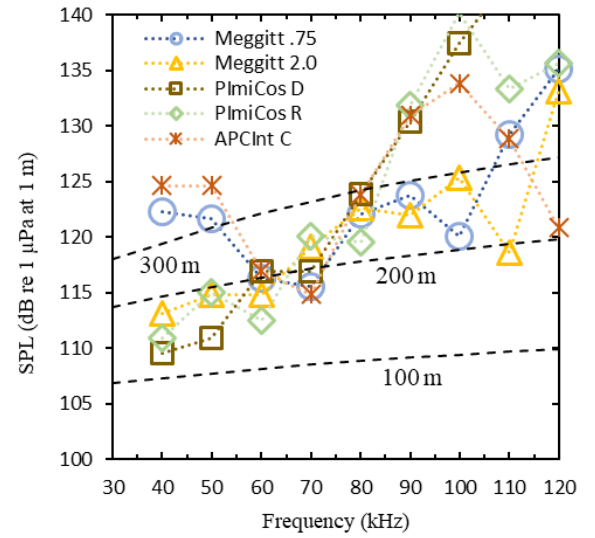


Fig. 8. Source level measurement for different piezoelectric transducers, which was tested at different frequencies and using a voltage amplitude of 6 Vp.
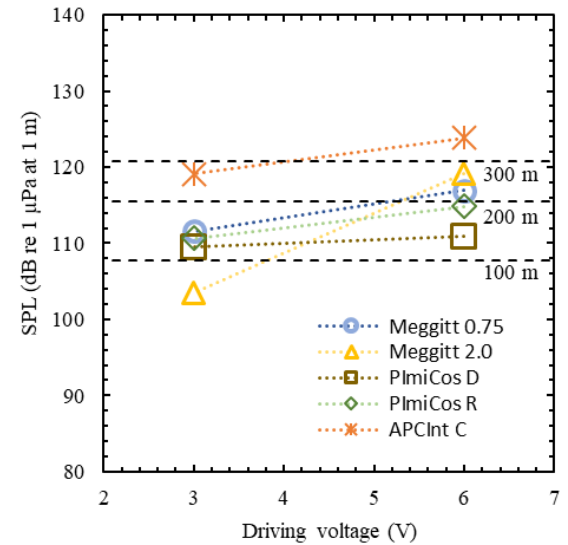


Fig. 9. Source level measurement for different piezoelectric transducers, which was tested at different voltage amplitudes and using a 50 kHz signal.

From these results, we can observe that an optimal frequency around 50 kHz is appreciable in Meggitt.75 and Cylinder devices at 6 Vp (i.e. there is a maximum in the measured SL). Though, the voltage provided by the piezoelectric driver (3 Vp) is enough to attain the SL threshold of 115.5 dB re 1 μPa at 1 m for the Cylinder.

## V. CONCLUSIONS

This work describes the basis and the preliminary laboratory tests of a new bidirectional acoustic tag. The bidirectional capability permits *in situ* reprogramming and range measurements between the tag and the receiver. The first laboratory test presented in this study shows that the signal level and frequency response will allow transmissions of at least 200 m, which it is a typical value for those small tags. In addition, the initial tests show a life time of 80 days in Polling mode configuration. Nonetheless, more tests have to be conducted in marine environments to investigate the real piezoelectric transducers performance in real conditions.

## REFERENCES

[1] J. Aguzzi, N. Bahamon, and L. Marotta, "The influence of light availability and predatory behavior of the decapod crustacean Nephrops norvegicus on the activity rhythms of continental margin prey decapods," *Mar. Ecol.*, vol. 30, no. 3, pp. 366–375, 2009, doi: 10.1111/j.1439-0485.2008.00276.x.

[2] D. Cote *et al.*, "Characterizing snow crab (Chionoecetes opilio) movements in the sydney bight (Nova Scotia, Canada): A collaborative approach using multiscale acoustic telemetry," *Can. J. Fish. Aquat. Sci.*, vol. 76, no. 2, pp. 334–346, 2019, doi: 10.1139/cjfas-2017-0472.

[3] B. A. Block *et al.*, "Tracking apex marine predator movements in a dynamic ocean," *Nature*, vol. 475, no. 7354, pp. 86–90, Jul. 2011, doi: 10.1038/nature10082.

[4] G. C. Hays *et al.*, "Translating Marine Animal Tracking Data into Conservation Policy and Management," *Trends Ecol. Evol.*, vol. 34, no. 5, pp. 459–473, 2019, doi: 10.1016/j.tree.2019.01.009.

[5] J. E. Edwards, J. Pratt, N. Tress, and N. E. Hussey, "Thinking deeper: Uncovering the mysteries of animal movement in the deep sea," *Deep Sea Res. Part I Oceanogr. Res. Pap.*, vol. 146, no. February, pp. 24–43, Apr. 2019, doi: 10.1016/j.dsr.2019.02.006.

[6] I. Masmitja *et al.*, "Mobile robotic platforms for the acoustic tracking of deep-sea demersal fishery resources," *Sci. Robot.*, vol. 5, no. eabc3701, 2020.

[7] W. W. L. Cheung *et al.*, "Large-scale redistribution of maximum fisheries catch potential in the global ocean under climate change," *Glob. Chang. Biol.*, vol. 16, no. 1, pp. 24–35, 2010, doi: 10.1111/j.1365-2486.2009.01995.x.

[8] S. O. Material, N. York, and A. Nw, "Change and Ocean Acidification," *Science (80-. )*., vol. 1737, no. December 2007, pp.

[9] A. C. Tsikliras, A. Dinouli, V. Z. Tsiros, and E. Tsalkou, "The Mediterranean and Black Sea fisheries at risk from overexploitation," *PLoS One*, vol. 10, no. 3, pp. 1–19, 2015, doi: 10.1371/journal.pone.0121188.

[10] B. Jin, X. Xu, and T. Zhang, "Robust time-difference-of-arrival (Tdoa) localization using weighted least squares with cone tangent plane constraint," *Sensors (Switzerland)*, vol. 18, no. 3, 2018, doi: 10.3390/s18030778.

[11] J. M. Nassar *et al.*, "Compliant lightweight non-invasive standalone 'Marine Skin' tagging system," *npj Flex. Electron.*, vol. 2, no. 1, pp. 1–9, 2018, doi: 10.1038/s41528-018-0025-1.

[12] T. A. Mooney, K. Katija, K. A. Shorter, T. Hurst, J. Fontes, and P. Afonso, "ITAG: An eco-sensor for fine-scale behavioral measurements of soft-bodied marine invertebrates," *Anim. Biotelemetry*, vol. 3, no. 1, pp. 1–14, 2015, doi: 10.1186/s40317-015-0076-1.

[13] H. Li, Z. D. Deng, Y. Yuan, and T. J. Carlson, "Design parameters of a miniaturized piezoelectric underwater acoustic transmitter," *Sensors (Switzerland)*, vol. 12, no. 7, pp. 9098–9109, 2012, doi: 10.3390/s120709098.

[14] M. S. Afzal, H. Shim, and Y. Roh, "Design of a piezoelectric multilayered structure for ultrasound sensors using the equivalent circuit method," *Sensors (Switzerland)*, vol. 18, no. 12, 2018, doi: 10.3390/s18124491.

[15] I. Masmitja *et al.*, "Range-Only Single-Beacon Tracking of Underwater Targets from an Autonomous Vehicle: From Theory to Practice," *IEEE Access*, vol. 7, pp. 86946–86963, 2019, doi: 10.1109/ACCESS.2019.2924722.

[16] I. Masmitja *et al.*, "Optimal path shape for range-only underwater target localization using a Wave Glider," *Int. J. Rob. Res.*, vol. 37, no. 12, pp. 1447–1462, 2018, doi: 10.1177/0278364918802351.

[17] K. M. Awan, P. A. Shah, K. Iqbal, S. Gillani, W. Ahmad, and Y. Nam, "Underwater Wireless Sensor Networks: A Review of Recent Issues and Challenges," *Wirel. Commun. Mob. Comput.*, vol. 2019, 2019, doi: 10.1155/2019/6470359.

[18] C. Coquet, C. Aubry, A. Arnold, and P.-J. Bouvet, "A Local Charged Particle Swarm Optimization to track an underwater mobile source," pp. 1–7, 2019, doi: 10.1109/oceanse.2019.8867527.

[19] D. Miorandi and S. Vitturi, "Analysis of master-slave protocols for real-time industrial communications over IEEE802.11 WLANs," *2nd IEEE Int. Conf. Ind. Informatics, INDIN'04*, pp. 143–148, 2004, doi: 10.1109/indin.2004.1417318.

[20] Y. Igarashi, R. Nakano, and N. Wakamiya, "A polling-based transmission scheme using a network traffic uniformity metric for industrial IoT applications," *Sensors (Switzerland)*, vol. 19, no. 1, 2019, doi: 10.3390/s19010187.

[21] D. Corregidor, I. Masmitja, J. M. López, S. Gomariz, J. Navarro, and G. de Arcas, "Analysis and initial design of bidirectional acoustic tag modulation schemes and communication protocol," in *IEEE International Instrumentation and Measurement Technology conference (I2MTC)*, 2021.

[22] L. APC International, *Piezoelectric Ceramics: Principles and Applications*, 2nd ed. 2011.

[23] F. B. Jensen, W. A. Kuperman, M. B. Porter, and H. Schmidt, *Computational Ocean Acoustics*. 2011.

[24] R. J. Urick, *Sound Propagation in the Sea*. 1979.

1737–1743, 2007, doi: 10.1126/science.1152509.